Actin-related protein2/3 complex regulates tight junctions and terminal differentiation to promote epidermal barrier formation

Kang Zhou[a,1], Andrew Muroyama[a,1], Julie Underwood[a], Rebecca Leylek[a], Samriddha Ray[a], Scott H. Soderling[a,b], and Terry Lechler[a,c,2]

Departments of [a]Cell Biology, [b]Neurobiology, and [c]Dermatology, Duke University Medical Center, Durham, NC 27710

Edited by Joan S. Brugge, Harvard Medical School, Boston, MA, and approved August 19, 2013 (received for review May 3, 2013)

The epidermis provides an essential seal from the external environment and retains fluids within the body. To form an effective barrier, cells in the epidermis must form tight junctions and terminally differentiate into cornified envelopes. Here, we demonstrate that the branched actin nucleator, the actin-related protein (Arp)2/3 complex, is unexpectedly required for both these activities. Loss of the ArpC3 subunit of the Arp2/3 complex resulted in minimal changes in the morphogenesis and architecture of this stratified squamous epithelium, but resulted in profound defects in its physiology. Mutant embryos did not develop an effective barrier to the external environment and died within hours of birth. We discovered two underlying causes for these effects. First, ArpC3 was essential for robust assembly and function of tight junctions, specialized cell–cell adhesions that restrict water loss in the epidermis. Second, there were defects in differentiation of the epidermis and the production of cornified envelopes, structures essential for barrier activity. Underlying this defect, we found that YAP was inappropriately active not only in the ArpC3 mutant tissue, but also in cultured cells. Inhibition of YAP activity rescued the differentiation and barrier defects caused by loss of ArpC3. These results demonstrate previously unappreciated roles for the Arp2/3 complex and highlight the functions of branched actin networks in a complex tissue.

The epidermis is a stratified squamous epithelium that forms a barrier between us and our environment. Although the 3D architecture of this tissue is required for its function, we have only a rudimentary understanding of how different cytoskeletal structures function to control tissue organization and physiology. The actin cytoskeleton is a dynamic structural component of the cell that is necessary for cell shape, migration, and adhesion. Because of its many roles, actin is essential and therefore cannot be studied by direct loss-of-function approaches. However, many proteins regulate the assembly, bundling, cross-linking, capping, severing, and disassembly of F-actin to generate diverse cytoskeletal structures. These include proteins that promote the nucleation of new actin filaments, such as the actin-related protein (Arp)2/3 complex, formins, and proteins with multiple G-actin binding motifs like cordon-bleu and Spire (1). Of these, the Arp2/3 complex is unique in that it promotes the formation of branched actin networks.

The mechanism and regulation of Arp2/3 complex-induced actin assembly has been extensively studied biochemically (2, 3). Cryo-EM and X-ray crystallography have yielded structural insights into the organization and interaction of the complex with actin filaments (4, 5). In addition, work in cultured cells has uncovered many Arp2/3 complex-dependent processes, including lamellipodia formation, efficient cell migration, endocytosis, vesicle trafficking, and adherens junction formation (6–10). Although the biochemistry and cell biology of the Arp2/3 complex have been well studied, most of our understanding of its role in intact tissues comes from invertebrate model systems. For example, the Arp2/3 complex is required for cell polarity and gastrulation in *Caenorhabditis elegans* embryos (11, 12). In *Drosophila*, the Arp2/3 complex plays roles in myoblast fusion, ring canal expansion, adherens junction formation, Notch signaling, and bristle development (6, 13, 14).

The functions of the Arp2/3 complex in intact tissues during mammalian development and homeostasis have only begun to be addressed. Loss of the Arp2/3 complex globally results in early lethality at the blastocyst stage in mice (15). In the mouse oocyte, the Arp2/3 complex is required for asymmetric cell division through positioning of the mitotic spindle (16). Finally, specific deletion of ArpC3 from postmitotic neurons resulted in delayed defects in dendritic spine morphology and schizophrenia-like phenotypes (17). These studies highlight that loss of the Arp2/3 complex in a tissue-specific manner can uncover unexpected roles for branched actin networks.

We wished to determine the roles of the Arp2/3 complex in the development and function of the epidermis, a stratified squamous epithelium. This tissue contains polarized cuboidal progenitor cells that undergo asymmetric cell divisions to form a multilayered, differentiated tissue that acts as a barrier to the external environment. Full barrier activity requires tight junction formation in the granular layer of the epidermis and the differentiation of cells into cornified envelopes that form the outer layer of the skin. Epidermal cells form robust adhesions to each other and to the underlying basement membrane and provide a physiological tissue context to analyze Arp2/3 function. We therefore generated mice with epidermal ablation of ArpC3, a peripheral subunit of the Arp2/3 complex required for robust F-actin nucleation. We find that ArpC3 is not required for cell shape, cell adhesion, or proper development of the 3D architecture of the epidermis. Unexpectedly, however, we find roles for ArpC3 in tight junction assembly and function and in YAP-mediated

Significance

This study used a genetic approach to probe the function of the F-actin nucleating Arp2/3 complex in skin development. Although the Arp2/3 complex was expected to be involved in morphogenesis and cell adhesion, loss of its activity did not result in architectural problems in the epidermis. However, Arp2/3 was essential for epidermal function. We revealed two unexpected functions for the Arp2/3 complex in the epidermis that are critical for tissue physiology: tight junction assembly/function and the regulation of YAP activity.

Author contributions: T.L. designed research; K.Z., A.M., J.U., R.L., S.R., and T.L. performed research; S.H.S. contributed new reagents/analytic tools; K.Z., A.M., J.U., R.L., S.R., and T.L. analyzed data; and T.L. wrote the paper.

The authors declare no conflict of interest.

This article is a PNAS Direct Submission.

[1]K.Z. and A.M. contributed equally to this work.

[2]To whom correspondence should be addressed. E-mail: terry.lechler@duke.edu.

This article contains supporting information online at www.pnas.org/lookup/suppl/doi:10.1073/pnas.1308419110/-/DCSupplemental.

differentiation of the epidermis, highlighting specific roles for core cell biological machinery in tissue physiology.

Results

Epidermal Ablation of ArpC3 Results in Perinatal Lethality with Barrier Defects but Largely Normal Tissue Architecture. To define Arp2/3 complex functions in the epidermis, we took advantage of a recently created ArpC3 floxed mouse line (17). Use of keratin 14 (K14) promoter–driven expression of Cre recombinase resulted in ArpC3 ablation from epidermal progenitors and their progeny during embryogenesis [referred to as ArpC3 conditional knockout (cKO)]. The K14-Cre transgene is expressed at approximately embryonic day (E) 13.5 and results in protein loss by E15.5, early in the stratification of the epidermis (18). Although present at expected Mendelian ratios in late embryogenesis, all ArpC3 cKO pups died within hours of birth. Despite this, it was not possible to distinguish ArpC3 cKO embryos from WT littermates from their gross appearance at E18.5, 1 d before birth. Animals did not exhibit any outward signs of tissue defects: no open eyes (a common phenotype in cytoskeletal and cell adhesion mutants) and no blistering of the skin. To determine whether ArpC3 was lost in the tissue, we isolated epidermal lysates and performed Western blot analysis for the protein. ArpC3 was clearly absent in the cKO tissue but easily detected in WT littermates (Fig. 1*A*). Histologic analysis of sections of WT and ArpC3 cKO back skin demonstrated that a stratified squamous epithelium developed quite normally in the mutant embryos (Fig. 1 *B–E*). We did not note any separations between the epidermis and the basement membrane or between cells, demonstrating that cell adhesion was not dramatically disrupted. Not only was the tissue intact, but we were also not able to detect any significant level of apoptosis in the mutant epidermis, as assayed by active caspase-3 staining (Fig. 1 *F* and *G*). Although the interfollicular epidermis looked remarkably normal, we did note areas of slight thickening of the epidermis and a decrease in the thickness of the terminally differentiated cornified layer (Fig. 1 *D* and *E*). There was also a decrease in the number of hair follicles in the ArpC3 cKO (20 ± 2 and 9 ± 2 follicles per 10× field of view for WT and cKO, respectively). Therefore, ArpC3 is not essential for stratification or cell viability in the epidermis and does not dramatically affect the rate of apoptosis.

To determine whether we could visualize any changes in F-actin organization or content in ArpC3 cKOs, we stained tissue sections with fluorescent phalloidin. We were surprised to find that F-actin was still present in ArpC3 cKO tissue at levels comparable to control. Closer examination, however, did reveal differences in its organization. In general, these changes reflected a decrease in cortical F-actin with an increase in cytoplasmic levels (Fig. 1 *I* and *J*). In basal cells, we observed increased perinuclear F-actin at the expense of cortical F-actin (Fig. 1 *K* and *L*). In granular layer cells, F-actin was less cortically enriched, and the cells appeared to have a more dense array of cytoplasmic filaments (Fig. 1 *M* and *N*). However, neither of these phenotypes was completely penetrant. This is likely in part because of the small size of the cytoplasm of these cells and our inability to image their organization with high resolution.

To determine whether ArpC3 loss affects actin organization in intact cells, we isolated *ArpC3* fl/fl keratinocytes from mice and used adenoviral-Cre transduction to induce ablation. Western blot analysis of lysates prepared 72 h after infection confirmed the absence of ArpC3 protein (Fig. 2*A*). We established stable clones from these cells and, where tested, the acute infection and the stable lines yielded the same results. In low-calcium media, in which cell–cell adhesions do not form and cells remain proliferative, ArpC3-null cells had many more filopodia-like structures on their basal surface (Fig. S1 *A–D*). In addition, strong perinuclear F-actin was also noted in the mutant cells compared with WT controls. The basal surface of the ArpC3-null cells also stained strongly for α-actinin and phospho-myosin light chain, both suggesting increased contractility (Fig. S1 *E–H*). Consistent with these structures being contractile, time-lapse movies of F-actin dynamics (using LifeAct-GFP transfected cells) revealed that regions at the base of ArpC3-null cells often lost their at-

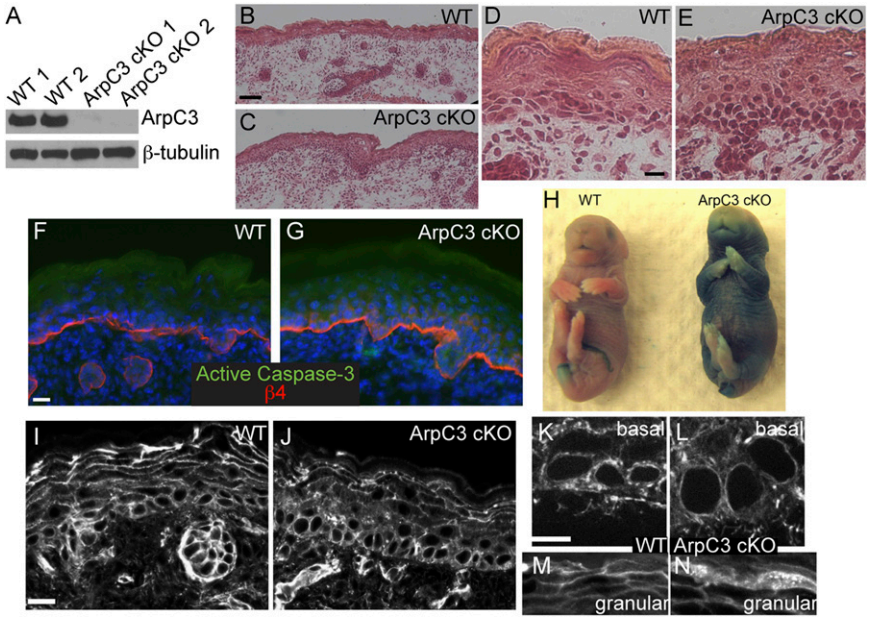

Fig. 1. Loss of ArpC3 in the epidermis results in barrier defects but only subtle changes in architecture and F-actin organization. (*A*) Western blot of ArpC3 and β-tubulin in lysates prepared from two WT and two ArpC3 cKO epidermises. (*B–E*) H&E-stained tissue sections from WT and ArpC3 cKO skin. (*F* and *G*) Immunofluorescence for active caspase 3 (green) and β4-integrin (red) in WT and ArpC3 cKO skin. β4-Integrin marks the junction between the dermis and the epidermis. (*H*) X-Gal barrier penetration assay in E18.5 WT and ArpC3 cKO embryos. The blue color indicates loss of barrier activity. (*I–N*) Rhodamine–phalloidin staining of F-actin structures in WT and ArpC3 cKO epidermis as indicated. (Scale bars: *B* and *C*, 50 μm; *D*, *E*, *I*, and *J*, 20 μm; 10 μm in *F, G, K,* and *L*.)

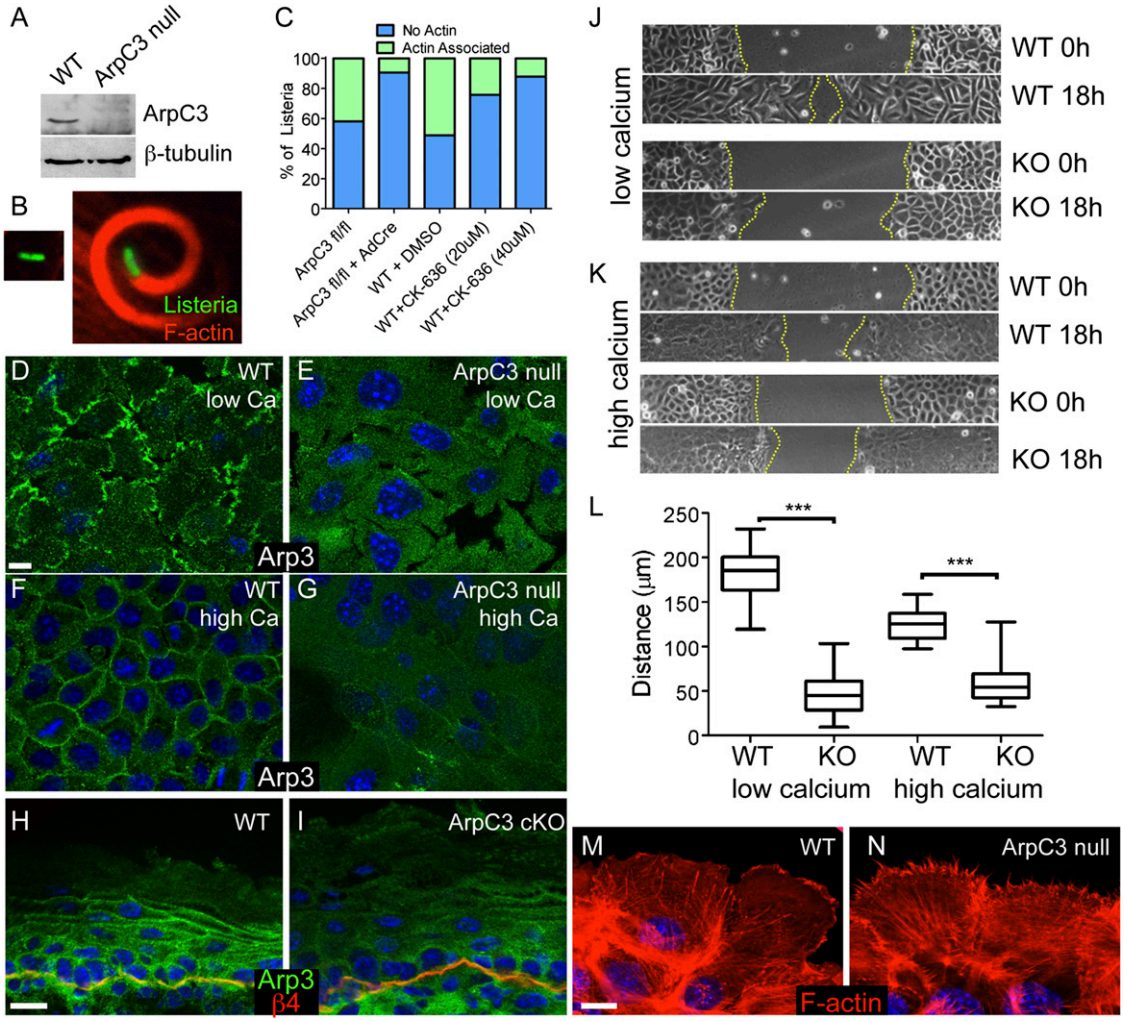

Fig. 2. Loss of ArpC3 results in defects in Arp2/3 complex activity and localization. (*A*) Western blot of ArpC3 and β-tubulin in lysates prepared from WT and ArpC3-null keratinocytes. (*B*) Examples of *Listeria* (green) that have not assembled actin around themselves (*Left*) or that have assembled F-actin (red; *Right*). (*C*) Quantification of *Listeria* actin assembly in control and ArpC3-null cells (ArpC3 fl/fl + AdCre) and in WT cells treated with the Arp2/3 inhibitor CK-636 ($P < 0.0001$ for ArpC3 fl/fl vs. ArpC3 fl/fl + AdCre and WT + DMSO vs. WT + CK-636 40 μM). (*D* and *E*) Arp3 localization in WT and ArpC3-null keratinocytes grown in low calcium containing media. (*F* and *G*) Arp3 localization in WT and ArpC3-null keratinocytes grown in 1.2 mM calcium-containing media. (*H* and *I*) Immunofluorescence of Arp3 (green) and β4-integrin (red) in WT and ArpC3 cKO epidermis. (*J*) Images of WT and ArpC3-null keratinocytes migrating into scratch wounds under low calcium conditions. (*K*) Images of WT and ArpC3-null keratinocytes migrating into scratch wounds in the presence of 1.2 mM calcium. (*L*) Quantification of migration rates of WT and ArpC3-null cells in low- and high-calcium conditions ($P < 0.0001$ for WT vs. KO under high- and low-calcium conditions). (*M* and *N*) F-actin organization at the leading edge of WT and ArpC3-null keratinocytes grown in 1.2 mM calcium-containing media. (Scale bars: 10 μm.)

tachment to the underlying substratum and snapped back into the cell (Fig. S1 *I* and *J*). Changes in the F-actin cytoskeleton were also noted when cells were grown in calcium-containing media, which allows cell-cell adhesion formation. Under these conditions, WT cells have F-actin bundles associated with cell–cell adhesions at the apical end of the cell and a web of F-actin at their base (Fig. S1 *K* and *M*). In ArpC3-null cells, the apical F-actin, although present, was at a lower intensity compared with the basal web (Fig. S1 *L* and *N*). In addition, whereas junctions between WT cells were quite straight, those in the mutant cells were more undulating. The localization of α-actinin was largely lost from the apical F-actin network in the mutant cells, although basal staining remained (Fig. S1 *O*–*R*). In total, these data demonstrate changes in F-actin organization in cultured ArpC3-null cells consistent with increased contractility at the basal surface and alterations in F-actin associated with cell–cell adhesions.

To better understand the underlying cause of perinatal lethality, we examined the ability of the epidermis to act as a barrier in E18.5 embryos. Isolated embryos were bathed in a solution containing X-Gal, which normally cannot penetrate the epidermis to stain the embryos (Fig. 1*H*). In ArpC3 cKO embryos however, the X-Gal penetrated the epidermis and turned the embryo blue, most prominently on the ventral surface. This lack of barrier activity is the likely cause of the lethality. Thus, although ArpC3 loss has surprisingly mild effects on the architectural appearance of the tissue, it is essential for epidermal function and barrier formation.

Loss of ArpC3 Results in Defects in F-Actin Assembly, Arp2/3 Localization, and Cell Migration in Cultured Keratinocytes. Previous work demonstrated that the Arp2/3 complex could be reconstituted without ArpC3, but it had a 12-fold decrease in actin nucleation activity in vitro (19). To examine in vivo Arp2/3 complex-dependent activity in ArpC3-null cells, we examined the ability of *Listeria*

monocytogenes to induce actin assembly in cells. We infected WT and ArpC3-null cells with GFP–*L. monocytogenes*, stained with fluorescent phalloidin to detect F-actin and quantified the number of bacteria capable of assembling F-actin clouds around themselves (Fig. 2 *B* and *C*). Although more than 40% of *Listeria* in control cells were able to assemble F-actin, less than 10% were able to do so in ArpC3 null cells. To compare ArpC3 loss to inhibition of Arp2/3 complex activity, we used two concentrations of the Arp2/3 inhibitor CK-636. At the higher dose, the drug produced inhibition near what we observed upon loss of ArpC3 (Fig. 2*C*). Both the levels of F-actin assembly on *Listeria* and the level of inhibition seen with drug treatment are similar to what was previously reported (20). These data demonstrate that loss of ArpC3 caused significant inhibition of Arp2/3 complex activity in keratinocytes.

Although Arp2/3 complex activity was largely lost in ArpC3-null keratinocytes, it was not clear whether other components of the Arp2/3 complex localized normally in the absence of ArpC3. In cultured keratinocytes grown in media with low levels of calcium (i.e., in the absence of robust cell–cell adhesions), Arp3, another component of the Arp2/3 complex, localized to membrane protrusions at the interface with the coverslip (Fig. 2*D*). This localization was lost in ArpC3-null cells (Fig. 2*E*). Upon addition of calcium to WT cells to induce cell–cell adhesion, Arp3 became prominently localized to sites of cell–cell contact (Fig. 2*F*). This localization was also significantly decreased in ArpC3-null cells (Fig. 2*G*). Although the loss of localization of Arp3 in the ArpC3-null cells is likely explained by loss of activity, we cannot rule out an additional direct role for ArpC3 in complex localization. The loss of Arp3 cortical localization was also noted in intact ArpC3 cKO epidermis (Fig. 2 *H* and *I*). In WT back skin, Arp3 was found in all layers of the epidermis. In basal and spinous layers, Arp3 appeared diffuse, and became more pronounced at cell–cell junctions in the granular cells of the epidermis. In ArpC3 cKO, the enrichment of Arp3 at junctions in the granular cells was decreased, consistent with our findings in cultured cells.

Finally, we performed scratch wound healing assays in cultured keratinocytes to examine the motile properties of ArpC3-null cells. ArpC3-null cells showed a marked defect in their rate of wound closure (Fig. 2 *J–L*). This was true in low-calcium conditions, in which cells migrated individually, and in high-calcium conditions, in which cells migrated as sheets. Wound edge morphology was distinct in ArpC3-null cells, exhibiting a spiky filopodial organization rather than the lamellipodia visualized in WT cells (Fig. 2 *M* and *N*), consistent with previous findings in fibroblast cells (7, 10). In total, these data demonstrate that loss of ArpC3 resulted in significant defects in Arp2/3 complex localization and activity in keratinocytes. Having established this, we sought to understand what roles the Arp2/3 complex plays in epidermal development and function.

ArpC3 Is Required for Tight Junction Assembly and Function. Although histological analysis did not reveal any major changes in cell–cell adhesion, previous studies in cultured cells have documented roles for the Arp2/3 complex in adherens junction assembly (8, 10, 21). However, examination of the localization of the adherens junction protein E-cadherin did not reveal any notable difference in the mutant epidermis (Fig. S2 *A* and *B*). To examine this more closely, we observed the kinetics of adherens junction formation in WT and ArpC3-null cells after addition of calcium to the media (Fig. S2 *C* and *D*). In this case, the cytoplasmic protein α-catenin, localized to the cell cortex with similar kinetics in WT and ArpC3-null cells. We next examined the turnover of α-catenin at the membrane by using fluorescence recovery after photobleaching (FRAP). The mobile fractions and recovery rates were similar between WT and ArpC3-null cells (Fig. S2 *E* and *F*). Although these results cannot rule out more subtle defects in adherens junctions, they do demonstrate that ArpC3 is not required for localization or stability of these cell adhesion structures in keratinocytes.

Because the ArpC3 cKO mice lacked a barrier and presumably died of dehydration, we next addressed the status of tight junctions. In tissue sections of the epidermis, we noted a decreased intensity and continuity of the tight junction protein ZO-1 (Fig. 3 *A* and *B*). To obtain a more complete view of tight junction architecture, we generated ArpC3 cKO embryos that also express ZO-1–GFP. The ZO-1–GFP is a knock-in strain that provides a sensitive and functional protein marker for tight junctions. By using whole-mount observations of the embryonic epidermis, we confirmed defects in tight junctions in the ArpC3 cKO animals (Fig. 3 *C* and *D*). In WT mice, whole-mount analysis revealed a regular cobblestone organization of tight junctions in the granular cells of the epidermis. In ArpC3 cKO mice, ZO-1–GFP intensity at the cell cortex was significantly diminished, and the signal was less contiguous. Ezrin/radixin/moesin (ERM) proteins are required for tight junction function in the epidermis (22). Ezrin showed markedly reduced junctional localization in the granular layers of the epidermis in ArpC3 cKOs (Fig. 3 *E* and *F*). Although these are more dramatic than the changes we noted in F-actin organization, the tight junction defects are likely caused by them.

We next turned to cultured keratinocytes, in which tight junction activity can be quantified. First, we determined whether there was a defect in tight junction morphology in ArpC3-null cultured keratinocytes. In WT cells, ZO-1 was found in straight junctions between cells (Fig. 3*G*). In ArpC3-null cells, ZO-1 was present, but the junctions were very wavy (Fig. 3*H*). We next tested the functional status of the tight junctions by measuring the transepithelial resistance (TER) of ArpC3-null and WT cells during a calcium switch. TER is a measure of the ability of an epithelial layer to restrict the flow of ions and is largely dependent on tight junctions. Although robust resistance was achieved within 36 h in WT cells, there was no significant increase in TER values for ArpC3-null cells even at 48 h (Fig. 3*I*). Therefore, in intact tissue and in cultured keratinocytes, ArpC3 loss resulted in tight junction perturbations.

Proliferation and Differentiation Defects in ArpC3 cKO Epidermis. Defects in tight junctions might contribute to the lethality and barrier defects observed. However, there is not a clear correlation between tight junction defects and outside-in barrier defects. For example, in E-cadherin cKO mice, tight junctions were perturbed but outside-in barrier activity (measured by X-Gal penetration) was normal (23). This is because the terminal differentiation products of the epidermis, the cornified envelopes and associated lipids provide an essential outside-in barrier. Disruption of tight junctions directly, as in the claudin 1-null mouse, resulted in clear inside-out barrier defects, but outside-in barrier activity was not measured (24). We therefore examined the ArpC3 cKO epidermis for additional defects.

The slightly thickened epidermis and decreased cornified layers suggested that proliferation/differentiation decisions may be altered in these embryos. To assess this, we examined the expression of keratin 5 (K5) and K14, markers for the proliferative basal progenitor cells. In WT back skin, K5 and K14 were largely restricted to the single layer of cells that sits on top of the basement membrane (Fig. 4*A*). In ArpC3 cKO epidermis, K5/14 positive cells were not restricted to the basal layer, being expanded into suprabasal layers (Fig. 4*B*). In WT epidermis, keratin 1 (K1), a marker of differentiated cells, was largely absent from basal cells, but was expressed throughout the differentiated suprabasal cell layers (Fig. 4*C*). This uniform expression was lost in the ArpC3 cKO, which exhibited a "salt-and-pepper" pattern of K1 staining in many areas (Fig. 4*D*). To continue examining the differentiation program in the epidermis, we assessed the expression of loricrin, a granular layer marker (Fig. 4*E*).

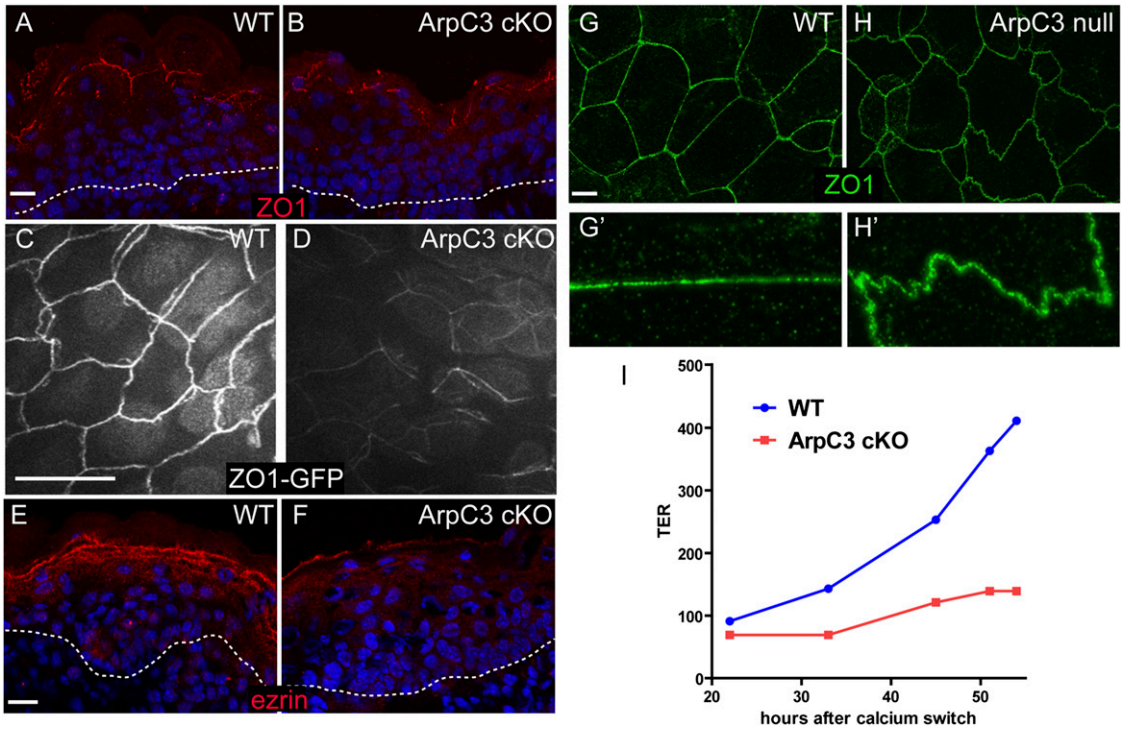

Fig. 3. Tight junction defects upon loss of ArpC3. (*A* and *B*) Immunofluorescence localization of the tight junction protein ZO-1 (red) in WT and ArpC3 cKO epidermis. The dotted line marks the basement membrane. (*C* and *D*) Epifluorescence of ZO1-GFP knock-in mice in the granular layer of the epidermis of WT and ArpC3 cKO embryos at E17.5. (*E* and *F*) Localization of ezrin (red) in the epidermis of WT and ArpC3 cKO epidermis. (*G* and *H*) ZO-1 organization in cultured WT and ArpC3-null keratinocytes. *G′* and *H′* highlight the difference in the linearity of the junctions. *G′* and *H′* are magnified views of areas of *G* and *H*, respectively. (*I*) Transepithelial resistance measurements for WT and ArpC3-null cells after a calcium switch. (Scale bars: *A*, *B*, and *E–I*, 10 μm; *C* and *D*, 50 μm.)

Loricrin expression was reduced and restricted to a smaller number of cell layers in ArpC3 cKO epidermis (Fig. 4*F*). Filaggrin, another marker for the granular layer, also showed decreased levels in the ArpC3 cKO epidermis by quantitative real time (RT)-PCR (qRT-PCR) analysis (Fig. 4*G*). In addition, isolation of cornified envelopes, the product of terminal differentiation in the epidermis, from E18.5 embryos revealed a 5× increase in abnormal and misshapen structures (6% in WT, 29% in ArpC3 cKO; $n > 150$). These data demonstrate that normal differentiation of the epidermis is perturbed upon ArpC3 loss.

The increase in K5/14-positive cells suggested an increase in proliferation in the ArpC3 cKO epidermis. We performed BrdU-incorporation analysis and quantified a more than twofold doubling in proliferating basal cells in the mutant (19 ± 3% for control and 42 ± 2% for ArpC3 cKO; $n > 200$; Fig. 4 *J* and *K*). As in WT epidermis, this proliferation was largely restricted to the basal cells that make direct contact with the underlying basement membrane. In addition, the hyperproliferation and stress marker, keratin 6 (K6), was dramatically up-regulated in the ArpC3 cKO epidermis (Fig. 4 *H* and *I*). In total, these data demonstrate that hyperproliferation and a block in differentiation resulted from loss of ArpC3 in the epidermis.

To better understand the underlying cause of these defects, we performed transcriptional profiling of WT and ArpC3 cKO epidermis. Analysis of microarray data from E17.5 WT and mutant epidermis demonstrated significant changes in a number of pathways. First, consistent with our studies on differentiation, we noted a decrease in the levels of many epidermal differentiation genes (such as loricrin and filaggrin), especially those associated with the granular layer (Table 1). At the same time, Sprr genes, which respond to barrier loss, were up-regulated in the ArpC3 cKO samples (25, 26). Consistent with the defects in tight junction and barrier formation, a large number of wound healing and migration genes were also up-regulated. In addition to these, we found two groups of up-regulated genes that we examined in more detail because of their roles in proliferation and differentiation decisions in the epidermis. These included components of the EGFR signaling pathway and YAP target genes.

EGF Ligand Up-Regulation in ArpC3 cKO Epidermis. Microarray analysis demonstrated that six EGF receptor ligands, all except EGF itself, were significantly up-regulated in ArpC3 cKO epidermis (Table 1). This increase in expression was validated by qRT-PCR analysis (Fig. S3*A*). Of these, epigen (>40×) and amphiregulin (>8×) were the most highly induced. Because increased signaling through tyrosine kinase receptors leads to activation of Jun through phosphorylation, we examined the levels of pJun in WT and ArpC3 cKO epidermis. A dramatic increase in pJun levels was observed in the mutant (Fig. S3 *B* and *C*). Consistent with this, we noted increased pJun levels by Western blot analysis (Fig. S3*D*). To determine whether changes in Jun activation required the tissue context or whether they were cell-autonomous, we examined pJun levels in WT and ArpC3-null keratinocytes. No differences were noted between the two cell lines, demonstrating that these alterations are tissue context-dependent (Fig. S3*E*). However, activation of this pathway likely contributes to the in vivo hyperproliferation phenotype.

Increase in YAP Activity in ArpC3 cKO Epidermis and Cultured Cells. YAP target genes were up-regulated in the ArpC3 cKO epidermis by transcriptional profiling (Table 1). YAP is responsive to changes in cell adhesion and cell mechanics (27). Hyperactivation of YAP drives proliferation and inhibits differentiation in the epidermis, leading to tumor formation in mice (28–30). To examine the contribution that the YAP pathway makes to the ArpC3 phenotype, we began by validating the RNA levels

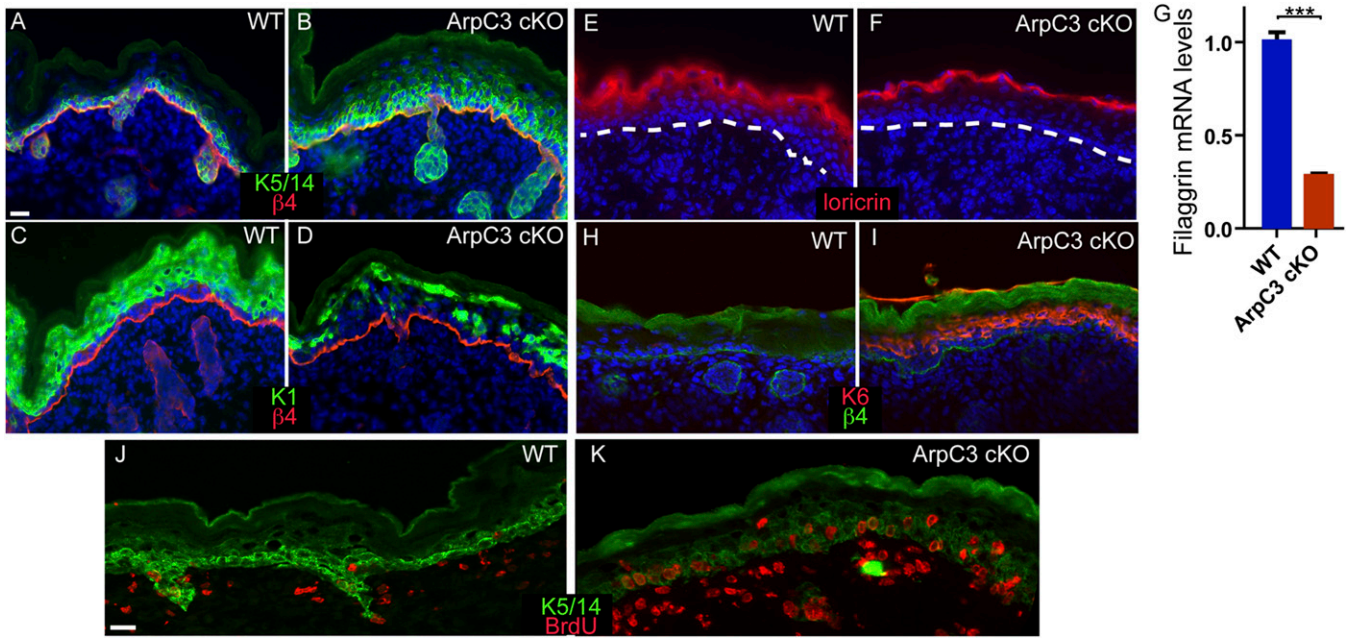

Fig. 4. Differentiation defects in ArpC3 cKO epidermis. (*A* and *B*) Immunofluorescence localization of K5/14 (green) and β4-integrin (red) in WT and ArpC3 cKO epidermis. (*C* and *D*) Localization of K1 (green) in the epidermis of WT and ArpC3 cKO embryos. (*E* and *F*) Loricrin protein localization (red) in WT and ArpC3 cKO epidermis. The dashed line indicates the basement membrane. (*G*) Quantitative PCR (qPCR) analysis of levels of filaggrin mRNA in WT and ArpC3-null epidermis ($P < 0.0001$). (*H* and *I*) K6 (red) expression in WT and ArpC3 cKO epidermis. (*J* and *K*) BrdU-incorporating cells (red) were visualized by anti-BrdU staining of WT and ArpC3 cKO skin sections. Dams were injected with BrdU 1 h before euthanasia and collection of embryos.

of three YAP target genes by qRT-PCR analysis. Cyr61, CTGF, and CCRN4L were significantly up-regulated, consistent with the microarray results (Fig. 5*A*). YAP activation involves its translocation into the nucleus and its association with TEAD factors. To validate increased YAP association with TEAD factors, which is required for downstream target expression, we immunoprecipitated YAP from WT and ArpC3-null cells and examined immunoprecipitates for levels of TEAD. Consistent with increased YAP activity, we noted increased association of YAP with TEADs in the ArpC3-null cells (Fig. 5*B*).

Nuclear translocation of YAP serves as a sensitive readout for pathway activity. In WT mice, more than 40% of basal cells had nuclear YAP (Fig. 5 *C* and *E*). In ArpC3 cKO epidermis, this number increased to more than 60% (Fig. 5 *D* and *E*). Again, we wanted to know whether these effects were a tissue context-dependent or whether they could be recapitulated in cultured cells. We therefore examined YAP localization in cultured WT and ArpC3-null cells at high confluence. High confluence was necessary because subconfluent cells have high levels of nuclear YAP. Under these conditions, we observed a large increase in nuclear YAP in ArpC3-null cells compared with WT cells (Fig. 5 *F–H*). This effect did not depend on cell adhesions, as it was observed in high- and low-calcium conditions. These data demonstrate that the effects of YAP are a direct response to loss of ArpC3 and are not secondary to tissue defects and the wound healing response. This effect is not mediated through defective adherens junctions as the phenotype is seen even in the absence of these structures. However, nuclear YAP localization in the ArpC3-null cells was lost after treatment with latrunculin A to perturb F-actin organization (Fig. 5*H*) or with blebbistatin to inhibit myosin II contractility (Fig. 5*I*).

YAP Inhibition Rescues Differentiation Defects of ArpC3 cKO Embryos. Although constitutive activation of YAP causes hyperproliferation and tumor formation (28–30), it was not clear how the more moderate increase in YAP activation observed in ArpC3 cKO embryos affects epidermal development. To determine whether the phenotypes associated with ArpC3 loss could be ameliorated by decreasing YAP pathway activity, we injected pregnant dams with the YAP inhibitor verteporfin at E17.5 and examined embryos at E18.5 (31). To validate efficacy of inhibition, we prepared RNA from treated embryos and examined YAP target gene expression by qRT-PCR. There was a significant and almost complete rescue of three previously mentioned YAP target genes, demonstrating that the inhibitor was functioning (Fig. 6*A*). We therefore went on to examine phenotypes in these mice.

Table 1. Microarray results

Category	Gene name (fold change by microarray)
Wound healing/migration	K6a (68), K6b (38), K16 (22), S100a8 (19), S100a6 (4), S100a9 (54), TSLP (188), TenC (5), Mmp3 (7), Adamts1 (2), Adam8 (3), Adamts (10), Coll8a1 (3), Coll4a1 (3), Zyx (2), FN1 (2), Pxn (2), Lamc1/Lamb1/Lama5 (2)
EGFR signaling	Areg (3), Ereg (2), Epgn (18), Tgfa (3), Hbegf (2), Btc (2), Jun (4), Junb (2)
YAP target genes	Cyr61 (2), CCRN4l (2), CTGF (2), FLNA (2), FSCN1 (2), GLIS2 (2), SDPR (2), ANLN (2), AXL (2), ETV5 (2), FSTL1 (2), MACF1 (2), SCHIP1 (2), SERPINE1 (2), TGFB2 (2), TSPAN3 (2)
Barrier loss response	Sprr1a (11), Sprr2h (10), Sprr1b (5), Sprr2d (4), Sprr2a1 (2)
Down-regulated differentiation genes	Lor (2), Fig (2), Tgm3 (2), Cdsn (2), Dsc1 (2), Tjp3 (3), ArpC3 (control; down 4)

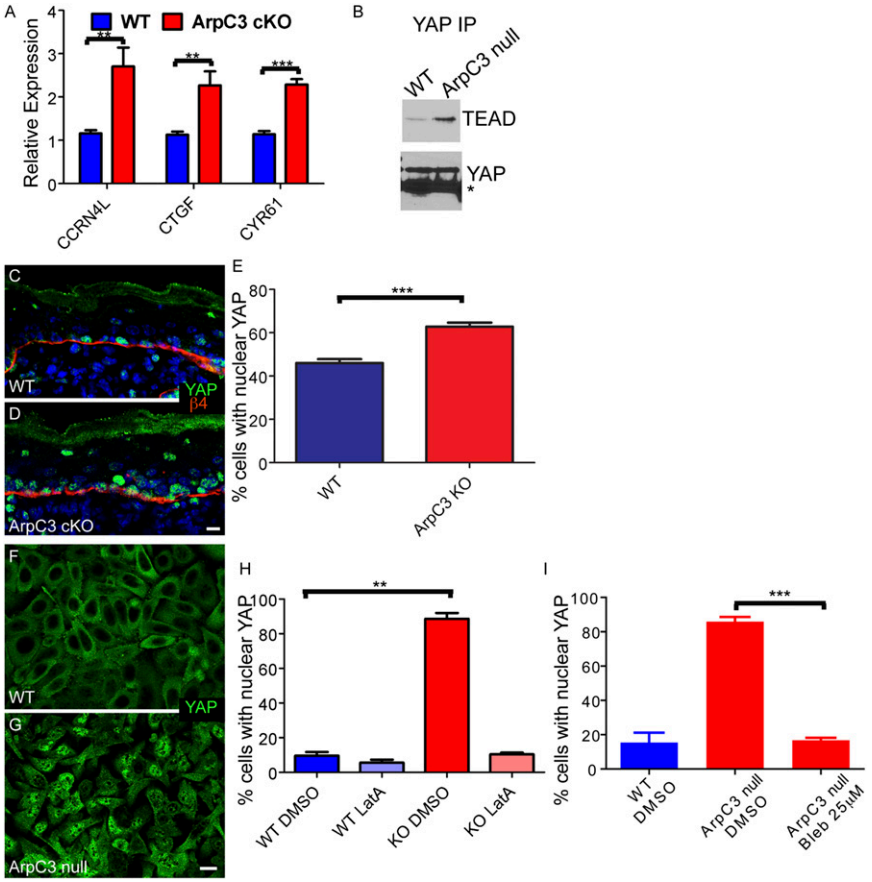

Fig. 5. YAP activation upon loss of ArpC3. (*A*) qPCR analysis of the levels of three YAP target genes: CCRN4L, CTGF, and CYR61. RNA was collected from E18.5 embryos. *P* values for the differences are 0.0029, 0.0033, and <0.0001, respectively. (*B*) Cell extracts from WT or ArpC3-null cells were immunoprecipitated with anti-YAP antibodies. Bound proteins were examined by Western blot analysis. (*C* and *D*) Immunofluorescence localization of YAP (green) in WT and ArpC3 cKO epidermis. (*E*) Quantification of the number of basal cells with nuclear YAP in WT and ArpC3 cKO embryos. The ArpC3 cKO had a significant increase in cells with nuclear YAP ($P = 0.0005$, from $n = 3$ embryos and $n > 250$ cells counted per embryo). (*F* and *G*) Localization of YAP in confluent WT and ArpC3-null keratinocytes. (*H*) Quantification of cells with nuclear YAP grown under the indicated conditions. ArpC3-null cells had a significant increase in cells with nuclear YAP ($P = 0.004$, $n > 300$ cells from each of two independent experiments), and this effect was lost after disruption of F-actin with latrunculin-A. (*I*) Quantification of cells with nuclear YAP after treatment with the myosin II inhibitor blebbistatin. The inhibitor-treated ArpC3-null cells had a significant decrease in cells with nuclear YAP ($P = 0.0009$, $n > 300$ cells from each of two independent experiments). (Scale bars: 10 μm.)

YAP inhibition did not rescue the tight junction localization defect or the expression of the stress marker K6 (Fig. S4). In addition, pJun levels and proliferation rates were still increased after treatment (Fig. S4). However, there was a significant rescue of differentiation defects in the ArpC3 cKO embryos treated with verteporfin. The levels of K1 in the spinous layers of the epidermis were normalized, as was the expression of loricrin (Fig. 6 *C–F*; compare with Fig. 4 *C–F*). In addition, mRNA levels of filaggrin returned to normal (Fig. 6*B*). Because treatment of ArpC3 cKO embryos with verteporfin rescued the expression of terminal differentiation genes, we next asked whether the outside-in barrier defect was rescued by YAP inhibition. When verteporfin-treated embryos were subjected to the X-Gal dye barrier assay, we noted a substantial, although not complete, rescue of barrier activity (Fig. 6*G*). Although small areas were still barrier-defective, much of the embryos' surfaces had intact barrier function. Therefore, increased YAP activity upon loss of ArpC3 is responsible for terminal differentiation defects and barrier loss.

Discussion

We have characterized how loss of a component of the Arp2/3 complex affects a mammalian epithelial tissue. Our results were surprising in the lack of expected phenotypes and the presence of unanticipated defects in the epidermis. Even though the Arp2/3 complex is essential for epidermal function, it has little effect on the architecture of the tissue. Despite this, ArpC3 was necessary for two distinct aspects of epidermal barrier acquisition: tight junction function and terminal differentiation. In addition to these functions, there were additional phenotypes that depended upon the tissue context and were likely secondary to defects in tight junctions and/or barrier formation. These indirect effects included a wound healing-type response with increased expression of EGFR ligands and inflammatory signals, which likely mediates, in part, the hyperproliferation seen in the mutant embryos.

Although Arp2/3 complex activity is required for cell viability in yeast (32), epidermal cells are able to tolerate a substantial decrease in the activity of this actin nucleator. Not only do epidermal cells survive and proliferate in the absence of ArpC3, they form an epidermis with a largely normal morphology. Although it is possible that low levels of Arp2/3 activity may suffice for these functions, this is unlikely to be the case, as our data suggest that loss of ArpC3 has a dramatic effect on Arp2/3 activity and localization in intact cells. In addition, we noted no separations between cells or cells and the underlying basement

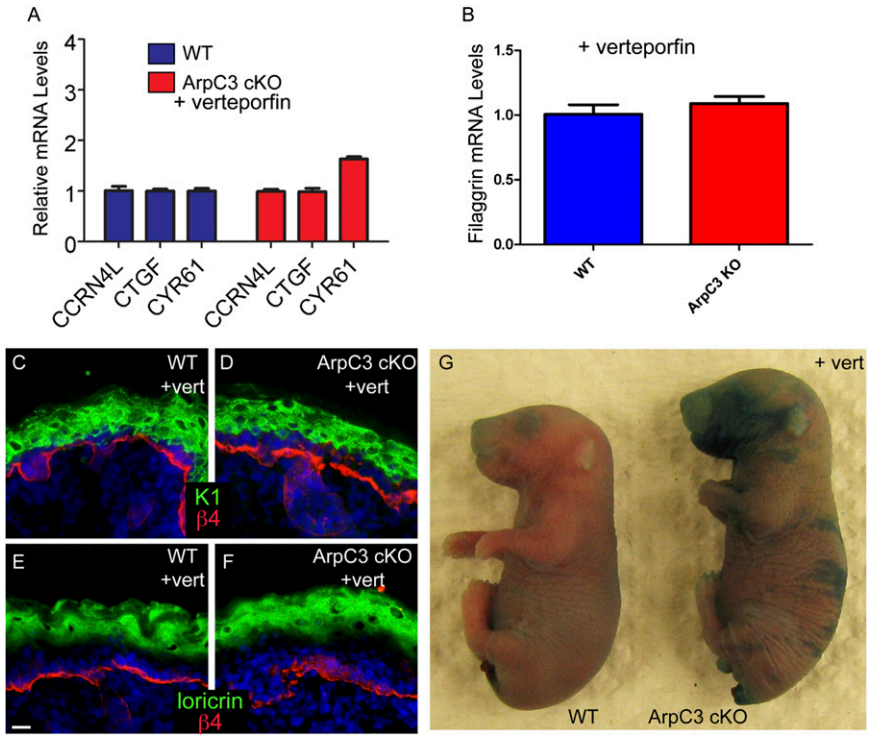

Fig. 6. YAP inhibition rescues terminal differentiation defects in the ArpC3 cKO epidermis. (*A*) qPCR analysis of three YAP target genes—CCRN4l, CTGF, and CYR61—in E18.5 epidermis from WT and ArpC3 embryos that were treated with verteporfin at E17.5 ($P = 0.44$, $P = 0.42$, and $P = 0.003$, respectively). (*B*) qPCR analysis of the levels of filaggrin mRNA in WT and ArpC3 cKO after verteporfin treatment. (*C* and *D*) Immunofluorescence localization of K1 (green) in WT and ArpC3 cKO epidermis after verteporfin treatment. (*E* and *F*) Localization of loricrin (green) in WT and ArpC3 cKO epidermis. (*G*) Barrier assay performed on E18.5 WT and ArpC3 cKO embryos that were treated with verteporfin at E17.5.

membrane, no increase in apoptosis and no defects in cell polarity or asymmetric cell divisions. Of these, we were most surprised by a lack of defects in cell–cell adhesion and adherens junction activity. A number of studies have suggested that Arp2/3-dependent actin assembly occurs at adherens junctions and is important for their assembly and function, at least in cultured cells (8, 10, 21). In contrast, we noted no defects in adherens junction assembly or turnover in epidermis or cultured keratinocytes. Formin proteins may be the essential or redundant nucleators of F-actin for adherens junction assembly in keratinocytes, as previously suggested (33).

Loss of ArpC3 resulted in a clear defect in tight junctions in vivo and in cultured cells. In intact tissue, the levels of the tight junction protein ZO-1 at the cell cortex and its continuity were decreased. This was noted by immunofluorescence against the endogenous protein and by using a fully functional ZO-1–GFP knock-in mouse model. Tight junctions were also defective in cultured cells as assayed based on morphology and by TER. There are a number of nonexclusive possibilities that may explain these findings. First, the Arp2/3 complex may directly generate F-actin structures that link to tight junction proteins such as ZO-1. Second, it may generate F-actin structures that recruit other proteins, such as ERM family members, that are required for tight junction function (22). Finally, it may be required for F-actin organization that allows productive tension to form on adherens junctions and tight junctions. In cultured cells, Arp2/3 complex activity has been reported to play a role in junctional tension (34). As tight junction assembly and activity is modulated by tension on adherens junctions, this may also contribute to the observed defects (35). Therefore, although we noted no obvious defects in adherens junctions localization or turnover, there may still be subtle defects that are physiologically important.

Loss of ArpC3 also resulted in an unexpected differentiation defect in the epidermis. Our data suggest that this is a result of inappropriate activation of the YAP transcription factor. This is supported by increased YAP nuclear localization in vivo and in cultured cells, increased association of YAP with its cofactor TEAD, and increased expression of YAP target genes. Pharmacologic inhibition of YAP activity specifically rescued the differentiation defects in the mutant embryos. This raises the question of why loss of Arp2/3 activity results in YAP activation. There are two likely possibilities based on known activators of YAP activity: either the pathway is directly sensitive to changes in F-actin organization or it is sensitive to changes in the mechanical properties of the cell. Our data have documented changes in F-actin organization in cultured ArpC3-null cells as well as changes consistent with increased contractility. Both disruption of F-actin and inhibition of contractility resulted in a loss of YAP nuclear localization, consistent with results in other cells (27). Although there are clear differences in F-actin organization in cultured cells, it has been more difficult to define the changes that occur in intact tissues, where cells are compact and the small cytoplasmic space contains a large nuclear volume. Therefore, although uncertainty still remains about the nature of the cytoskeletal changes in vivo, our data suggest that pathways that converge on Arp2/3-mediated F-actin assembly will affect YAP activity and epidermal differentiation.

In summary, the present study has revealed two unexpected functions for the Arp2/3 complex in the epidermis that are critical for tissue physiology: tight junction assembly/function and the regulation of YAP activity. Neither of these was suspected from biochemical studies or studies on cultured cells. This highlights the importance of examining the function of cell biological regulators in their native tissue context.

Methods

Mice. All mouse studies were performed with approval from the Institutional Animal Care and Use Committee of Duke University. K14-Cre (18) and ArpC3 fl/fl mice (17) have been described previously.

Antibodies and Staining. Antibodies used included rabbit anti-ArpC3 and mouse anti-Yap (Santa Cruz Biotechnology), mouse anti-Arp3, mouse anti-ezrin, rat anti-BrdU (Abcam), rabbit anti-active caspase 3 (R&D Systems), rabbit anti-Yap and rabbit anti–phospho-myosin light chain Thr18/Ser19 (Cell Signaling), rabbit anti–ZO-1 (Invitrogen), mouse anti–α-actinin (Sigma), rabbit anti-K6 (Covance), rat anti–β-4 integrin, mouse anti-TEAD (BD), rabbit anti-K1 (gift from Colin Jamora, University of California, San Diego), and chicken anti-K5/14 (laboratory-generated). Cells or tissue sections were fixed with 4% (wt/vol) paraformaldehyde for 8 min at 37 °C or in −20 °C methanol for 2 min. Blocking was performed with PBS solution with 0.1% Triton X-100 containing 5% (wt/vol) normal goat serum, 5% (wt/vol) normal donkey serum, and 3% (wt/vol) BSA (Sigma). For experiments using mouse antibodies on mouse tissues, MOM block (Vector Labs) was used according to the manufacturer's instructions. Secondary antibodies were Alexa 488-labeled (Invitrogen) and Rhodamine Red-X–labeled (Jackson ImmunoResearch). Samples were imaged with an Axio Imager Z1 microscope with Apotome attachment (Zeiss).

Barrier Assay. E18.5 embryos were collected and submerged in solution containing 1 mg/mL X-Gal, 100 mM $NaPO_4$, 1.3 mM $MgCl_2$, 3 mM $K_3Fe[CN]_6$, 0.01% sodium deoxycholate, and 0.2% Nonidet P-40. Staining was halted by washing in PBS solution when color had developed.

Cornified Envelope Preparation. Isolated E18.5 epidermis was minced with a razor blade and then boiled for 5 min in 2% (wt/vol) SDS with 10 mM Tris·HCl (pH 7.5), 5 mM EDTA, and 10 mM DTT. Resulting cornified envelopes were then examined on an Axiovert 40 microscope (Zeiss). At least 200 cornified envelopes were counted for each of two WT and ArpC3 cKO embryos.

In Vitro Wound-Healing Experiment. Cultured keratinocytes were grown to confluence in low calcium containing media and then wounded directly or switched into 1.2 mM containing calcium medium for 2 h before wounding. Scratch wounds were generated by scraping a pipette across the cell layer. Images were collected at 0 h and at 6 h time increments on an Axiovert 40 microscope (Zeiss).

TER. Cells were cultured to confluence on Costar Transwell Permeable membrane inserts. After addition of calcium to 1.2 mM, the TER was measured at various time points by using a Millipore Millicell ERS-2 ohmmeter. Readings were normalized against wells with no cells (set as zero resistance) and to insert area.

FRAP. For FRAP, WT and ArpC3-null mouse keratinocytes were plated onto 35-mm glass-bottom dishes (MatTek). An α-catenin–GFP plasmid was transfected into the keratinocytes by using Mirus reagents. Approximately 10 h after transfection, the media was replaced with media containing 1.2 mM Ca^{2+}. After 24 h in calcium-containing media, cells were mounted onto a Zeiss 710 inverted confocal microscope for imaging. Image acquisition and data analysis were performed as previously described (35).

***Listeria* Motility.** GFP-expressing *L. monocytogenes* were grown overnight at 30 °C in brain heart infusion broth with erythromycin. For infections of WT and ArpC3-null keratinocytes, *Listeria* was added directly to culture media. After allowing infection to proceed for 1 h, keratinocytes were washed several times with PBS solution and fresh DMEM plus 10% (wt/vol) FBS with 50 μg/mL gentamicin added to the cells. Keratinocytes were fixed after 6 h with 4% (wt/vol) PFA and stained with fluorescent phalloidin to visualize accumulated actin. To quantify *Listeria* infection following pharmacological inhibition of the Arp2/3 complex, 20 μM or 40 μM CK-636 was added to the keratinocyte media 1 h before *Listeria* infection. After *Listeria* infection proceeded for 1 h, the culture media was replaced with the addition of CK-636. Fixation and staining was carried out in an identical manner. *Listeria* were quantified as "actin-associated" if actin was visible around the bacterium or if the *Listeria* had nucleated an actin tail.

Gene Expression. Epidermis samples were isolated from back skin after 1 h Dispase treatment at 37 °C. Total RNA was extracted by using a Qiagen RNeasy mini kit. A SuperScript First-Strand Synthesis System (Invitrogen) was used to generate cDNA. We chose previously validated primer sequences (http://pga.mgh.harvard.edu/primerbank/) for all genes we assayed. GAPDH gene was used as internal control. Quantitative-comparative RT-PCR was performed on StepOne Plus Real-Time PCR System (Life Technologies) using SYBR green reagent (SensiMix SYBR and Fluorescein Kit; Bioline). For microarrays, RNA was purified in the same manner and submitted to the Duke Microarray Core Facility for processing and hybridization on Affymetrix arrays.

Drug Treatments. Cells were treated with DMSO, latrunculin A (20 μg/mL), or blebbistatin (50 μM) for 1 h, washed once with PBS solution, and then fixed with 4% paraformaldehyde for 8 min.

At stage E17.5, pregnant dams were injected with verteporfin suspended in PBS solution at a dosage of 100 mg/kg. BrdU was administered by i.p. injection 1 h before the embryos were killed at E18.5. The back skin of the embryos were divided into portions, one of which was embedded for immunostaining and the other of which was for RNA extraction. In independent experiments, whole embryos treated with Yap inhibitor were collected for barrier assays.

ACKNOWLEDGMENTS. We thank Jennifer Zhang and members of the laboratory of T.L. for advice and for comments on the manuscript. This work was funded by National Institutes of Health Grants R01-AR055926 (to T.L.) and R01-NS059957 (to S.H.S.) and by the March of Dimes (S.H.S.).

1. Firat-Karalar EN, Welch MD (2011) New mechanisms and functions of actin nucleation. *Curr Opin Cell Biol* 23(1):4–13.
2. Rotty JD, Wu C, Bear JE (2013) New insights into the regulation and cellular functions of the ARP2/3 complex. *Nat Rev Mol Cell Biol* 14(1):7–12.
3. Pollard TD (2007) Regulation of actin filament assembly by Arp2/3 complex and formins. *Annu Rev Biophys Biomol Struct* 36:451–477.
4. Robinson RC, et al. (2001) Crystal structure of Arp2/3 complex. *Science* 294(5547):1679–1684.
5. Volkmann N, et al. (2001) Structure of Arp2/3 complex in its activated state and in actin filament branch junctions. *Science* 293(5539):2456–2459.
6. Rajan A, Tien AC, Haueter CM, Schulze KL, Bellen HJ (2009) The Arp2/3 complex and WASp are required for apical trafficking of Delta into microvilli during cell fate specification of sensory organ precursors. *Nat Cell Biol* 11(7):815–824.
7. Suraneni P, et al. (2012) The Arp2/3 complex is required for lamellipodia extension and directional fibroblast cell migration. *J Cell Biol* 197(2):239–251.
8. Tang VW, Brieher WM (2012) α-Actinin-4/FSGS1 is required for Arp2/3-dependent actin assembly at the adherens junction. *J Cell Biol* 196(1):115–130.
9. Verma S, et al. (2004) Arp2/3 activity is necessary for efficient formation of E-cadherin adhesive contacts. *J Biol Chem* 279(32):34062–34070.
10. Wu C, et al. (2012) Arp2/3 is critical for lamellipodia and response to extracellular matrix cues but is dispensable for chemotaxis. *Cell* 148(5):973–987.
11. Xiong H, Mohler WA, Soto MC (2011) The branched actin nucleator Arp2/3 promotes nuclear migrations and cell polarity in the C. elegans zygote. *Dev Biol* 357(2):356–369.
12. Roh-Johnson M, Goldstein B (2009) In vivo roles for Arp2/3 in cortical actin organization during C. elegans gastrulation. *J Cell Sci* 122(pt 21):3983–3993.
13. Hudson AM, Cooley L (2002) A subset of dynamic actin rearrangements in Drosophila requires the Arp2/3 complex. *J Cell Biol* 156(4):677–687.
14. Richardson BE, Beckett K, Nowak SJ, Baylies MK (2007) SCAR/WAVE and Arp2/3 are crucial for cytoskeletal remodeling at the site of myoblast fusion. *Development* 134(24):4357–4367.
15. Vauti F, et al. (2007) Arp3 is required during preimplantation development of the mouse embryo. *FEBS Lett* 581(29):5691–5697.
16. Yi K, et al. (2011) Dynamic maintenance of asymmetric meiotic spindle position through Arp2/3-complex-driven cytoplasmic streaming in mouse oocytes. *Nat Cell Biol* 13(10):1252–1258.
17. Kim IH, et al. (2013) Disruption of Arp2/3 results in asymmetric structural plasticity of dendritic spines and progressive synaptic and behavioral abnormalities. *J Neurosci* 33(14):6081–6092.
18. Vasioukhin V, Degenstein L, Wise B, Fuchs E (1999) The magical touch: Genome targeting in epidermal stem cells induced by tamoxifen application to mouse skin. *Proc Natl Acad Sci USA* 96(15):8551–8556.
19. Gournier H, Goley ED, Niederstrasser H, Trinh T, Welch MD (2001) Reconstitution of human Arp2/3 complex reveals critical roles of individual subunits in complex structure and activity. *Mol Cell* 8(5):1041–1052.
20. Nolen BJ, et al. (2009) Characterization of two classes of small molecule inhibitors of Arp2/3 complex. *Nature* 460(7258):1031–1034.
21. Georgiou M, Marinari E, Burden J, Baum B (2008) Cdc42, Par6, and aPKC regulate Arp2/3-mediated endocytosis to control local adherens junction stability. *Curr Biol* 18(21):1631–1638.
22. Gladden AB, Hebert AM, Schneeberger EE, McClatchey AI (2010) The NF2 tumor suppressor, Merlin, regulates epidermal development through the establishment of a junctional polarity complex. *Dev Cell* 19(5):727–739.

23. Tunggal JA, et al. (2005) E-cadherin is essential for in vivo epidermal barrier function by regulating tight junctions. *EMBO J* 24(6):1146–1156.
24. Furuse M, et al. (2002) Claudin-based tight junctions are crucial for the mammalian epidermal barrier: a lesson from claudin-1-deficient mice. *J Cell Biol* 156(6): 1099–1111.
25. Huebner AJ, et al. (2012) Amniotic fluid activates the nrf2/keap1 pathway to repair an epidermal barrier defect in utero. *Dev Cell* 23(6):1238–1246.
26. Patel S, Kartasova T, Segre JA (2003) Mouse Sprr locus: A tandem array of coordinately regulated genes. *Mamm Genome* 14(2):140–148.
27. Dupont S, et al. (2011) Role of YAP/TAZ in mechanotransduction. *Nature* 474(7350): 179–183.
28. Schlegelmilch K, et al. (2011) Yap1 acts downstream of α-catenin to control epidermal proliferation. *Cell* 144(5):782–795.
29. Silvis MR, et al. (2011) α-Catenin is a tumor suppressor that controls cell accumulation by regulating the localization and activity of the transcriptional coactivator Yap1. *Sci Signal* 4(174):ra33.
30. Zhang H, Pasolli HA, Fuchs E (2011) Yes-associated protein (YAP) transcriptional coactivator functions in balancing growth and differentiation in skin. *Proc Natl Acad Sci USA* 108(6):2270–2275.
31. Liu-Chittenden Y, et al. (2012) Genetic and pharmacological disruption of the TEAD-YAP complex suppresses the oncogenic activity of YAP. *Genes Dev* 26(12):1300–1305.
32. Winter DC, Choe EY, Li R (1999) Genetic dissection of the budding yeast Arp2/3 complex: A comparison of the in vivo and structural roles of individual subunits. *Proc Natl Acad Sci USA* 96(13):7288–7293.
33. Kobielak A, Pasolli HA, Fuchs E (2004) Mammalian formin-1 participates in adherens junctions and polymerization of linear actin cables. *Nat Cell Biol* 6(1):21–30.
34. Verma S, et al. (2012) A WAVE2-Arp2/3 actin nucleator apparatus supports junctional tension at the epithelial zonula adherens. *Mol Biol Cell* 23(23):4601–4610.
35. Sumigray KD, Foote HP, Lechler T (2012) Noncentrosomal microtubules and type II myosins potentiate epidermal cell adhesion and barrier formation. *J Cell Biol* 199(3): 513–525.